Defense Technical Information Center Compilation Part Notice

ADP012355

TITLE: Transport Properties and Thermodynamic Processes for Liquid Fuels and Gas Mixtures of N2, O2, H2 and H2O

DISTRIBUTION: Approved for public release, distribution unlimited

This paper is part of the following report:

TITLE: 2nd International Workshop on Rocket Combustion Modeling: Atomization, Combustion and Heat Transfer held in Lampoldshausen, Germany on 25-27 Mar 2001

To order the complete compilation report, use: ADA402618

The following component part numbers comprise the compilation report:
ADP012355 thru ADP012373

TRANSPORT PROPERTIES AND THERMODYNAMIC PROCESSES FOR LIQUID FUELS AND GAS MIXTURES of N_2, O_2, H_2 and H_2O

I.A. Sokolova*, N.A. Slavinskaya, O.J. Haidn*****

*Institute for Mathematical Modeling Russian Academy of Science,
Miusskaya pl.4-A, 125047, Moscow, sokolova@imamod.ru
**Central Institute of Aviation (CIAM), Aviamotornaya st.2, Russia, 111250 Moscow, slan@orc.ru
***German Aerospace Center (DLR), Langer Grund, 74239 Lampoldshausen, oskar.haidn@dlr.de

Abstract

This report deals with problems of transport properties in gas dynamic flows at high pressures and densities and, in particular, with transport properties of Hydrogen, Nitrogen, Water and Oxygen. The behavior of these substances at high pressures and/or low temperatures is quite different from perfect gas behavior. Especially near its critical points or lines of phase changes, thermodynamic properties, equations of state and transport properties as well exhibit proper characters while the specified conditions are taking place. An overview of models in use to predict the transport properties for the species given above in various phase states is carried out and different theoretical approaches are investigated. A generalization of the models requires the knowledge of all these properties in the widest possible range of temperatures and pressures. Therefore, the inclusion of limiting states' data (dilute gas, saturation and melting regime) into a multi-property analysis is essential, especially while extending these correlations beyond the range of experimental data.
A novel method for the prediction of viscosity and thermal conductivity on the basis of an unique equation for gas and liquid is presented which bases on the model of effective kinetic diameter of hard spheres. Furthermore, the kinetic effects on the droplet surface under high ambient temperature are considered. Temperature and concentration jumps were used to describe non-equilibrium boundary conditions on an evaporating liquid oxygen (LOX) droplet. The influence of calculation errors on the values of these jumps is evaluated.

Introduction

The properties of matters in various phase states may be divided into two kinds, equilibrium properties and transport properties. A great progress has been made in the recent years in studying equilibrium properties, although inconsistency between calculated properties is often a problem in industrial thermophysical properties simulations because typically different prediction methods are used for different phase states. Hence, it may happen that equations for liquids are used for the prediction of properties in a region where the vapor pressure equation indicates a gas phase should be present. Therefore, a consistent method for the prediction of all the properties based on a single set of fundamental parameters is the most preferable. A generalized equation of state can be used accurately to predict equilibrium properties of fluids and dense gases.
Furthermore, transport properties of matters in different thermo-physical states are also important features required in various engineering design problems such as simulations of viscous flows through channels and combustion chambers of various technical devices such as flows in rocket engines, chemical reactors or shock tubes. The governing equations for these gasdynamic systems are the Navier-Stokes equations with mass diffusion, heat flux, pressure tensor expressions. All the coefficients in these equations have to be known precisely since they have a very strong influence on the accuracy and the consistency of the simulations.
The object of our investigations presented here is (1), to provide adequate thermo-physical property data, mainly transport properties, covering the largest possible range of temperatures and densities, and (2), to demonstrate a model of vaporization accounting for thermal non-equilibrium boundary conditions on the surface of a liquid droplet.

Thermodynamic properties

Under various boundary conditions different physical phases such as dense gases and liquids usually co-exist, i.e. the flow of a mixture of cold gaseous hydrogen, superheated steam and liquid oxygen in a cryogenic liquid rocket engine. Although mixtures of layers of liquids and dense gases may be treated as a continuum, the properties of substances under high pressure and low temperature are quite different from those of a perfect gas. Hence, thermodynamic properties, equations of state and transport properties as well have their particular characteristics at specific conditions.

The conventional interpretation of the specific characteristics of thermo-physical properties of matters under different boundary conditions of pressures and temperatures generally makes use of well-known phase diagram of states. Figures 1 and 2 shown typical phase diagrams for N_2 and H_2.

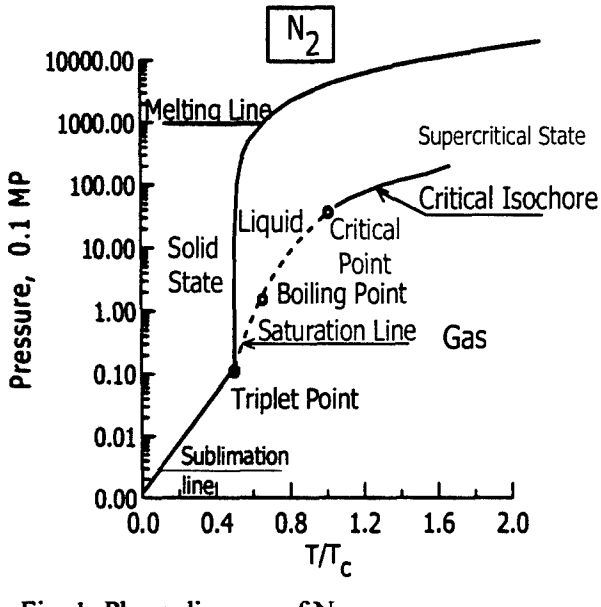

Fig. 1: Phase diagram of N_2

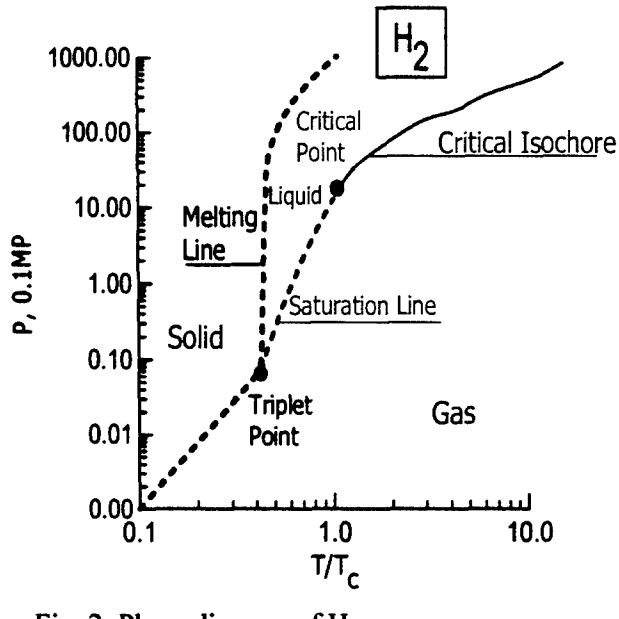

Fig. 2: Phase diagram of H_2

All three different physical phases: gas, liquid and solid states are realized under different pressures as the temperature varies. The triple point (TP) is the point of co-existence of all three phases. The melting line (ML) is the boundary line between the liquid and the solid state. The sublimation line separates the co-existence of gas and solid states. The saturation line (SL) is the boundary line between gas and liquid, along which specific volumes of gas and liquid co-exist at given temperatures and pressures. The critical point (CP) is characterized by the critical values of temperature T, pressure P and density ρ_c. The CP is the final point on the SL, where the density (or the specific volume) of a dense gas becomes equal to the density (or the specific volume) of a liquid. Above this point, phase transitions don't happen anymore. The distinctions between gas and liquid have all disappeared above CP, and the specific dense gas behavior is close to that of a liquid. In other words, it is impossible to distinguish between gas or liquid exists. The choice of boundary between gas and liquid has become a matter of convention and usually the critical isochore is used.

	$T_{melt.}$ K	$T_{boil.}$ K	$T_{crit.}$ K	$P_{crit.}$ $0.1MPa$	$\rho_{crit.}$ kg/m^3
p- H_2	13.8	20.28	32.98	12.93	31.4
n- H_2	13.95	20.38	33.23	13.16	31.6
N_2	63.15	77.35	126.25	33.96	304
O_2	54.35	90.18	154.60	50.9	406
Air			132.62	37.85	302.56
H_2O	273.	374.12	647.3	221.39	317.8

Table 1: Critical parameters of substances of interest

A brief summary of the critical parameters for some of the substances of interest is given in Table 1, much more details can be found in [1]. Although the critical parameters for various matters differ widely the particular behavior of thermodynamic (transport) properties near critical areas is quite similar.
Various papers have been devoted to the investigation of equations of state for simple fluid-gas substances such as H_2, O_2, N_2, or H_2O in wide ranges of temperature and pressure. The outcome of both experimental and theoretical treatments made it possible to work out accurate correlations for basic tables of thermodynamic properties, including specific volume (V), enthalpy (h), entropy (S), and specific thermal capacity (C_p) in terms of temperature T and pressure P, as unique reference sources of data [1][2][3]. As an example, the specific behavior of factor compressibility Z for Oxygen is shown in Figure 3, with p the pressure and V the specific volume.

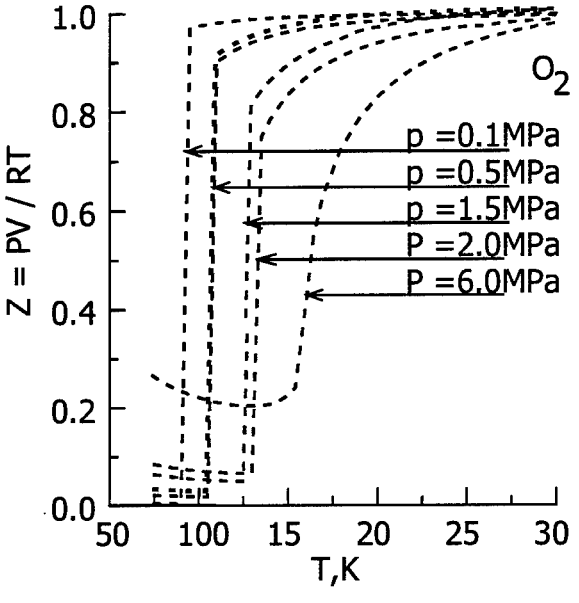

Fig. 3: Compressibility factor $Z = \frac{pV}{RT}$

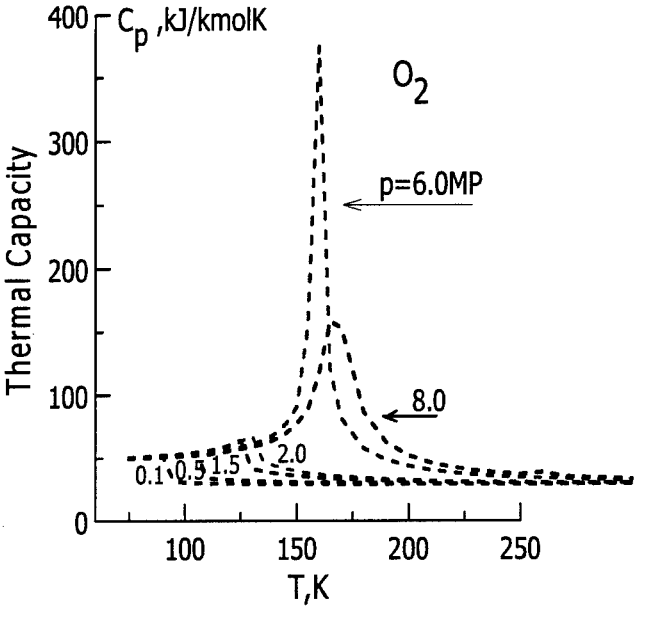

Fig. 4: Thermal Capacity near critical point

Near CP, a steep increase of the compressibility factor Z and an anomaly of the thermal capacity can be observed. Fluctuations in density, molar fractions and other physical values cause a delay of diffusion, a growth of viscosity and thermal conductivity and give rise to other problems. The thermodynamic properties near CP were investigated for H_2, O_2, N_2, and H_2O thoroughly and may be found in [1] or [3]. An example for the anomalous behavior of the specific thermal capacity of O_2 near critical region is shown in Figure 4.

Transport Properties

For dense gases, viscosity, thermal conductivity and thermal diffusion as well are the functions of temperature and pressure (density). Atypical diagram of the reduced viscosity η^* in terms of reduced density ρ^* and temperature T^* is shown on Figure 5. Areas of moderate dense gas (G) and liquid (L) are pointed out. The line relating to the diluted gas limit (DGL), the saturation line (SL) and the melting line (ML) are mapped on the diagram as the bounding lines of the $\eta^* - \rho^* - T^*$ surface. The picture clearly shows the complex behavior of the viscosity in terms of density and temperature.

Generally, analytical expressions are used for application oriented calculations. Hence, accurate correlations are needed. The analytical generalization of experimental data includes property data in the as wide as possible range of temperature and density. Therefore, data near critical areas, saturation line and melting are very important in any multi-property analysis, especially when the correlations are to be extended onto areas which lack experimental data. Additionally, data of viscosity and thermal conductivity in the dilute gas limit is needed as well.

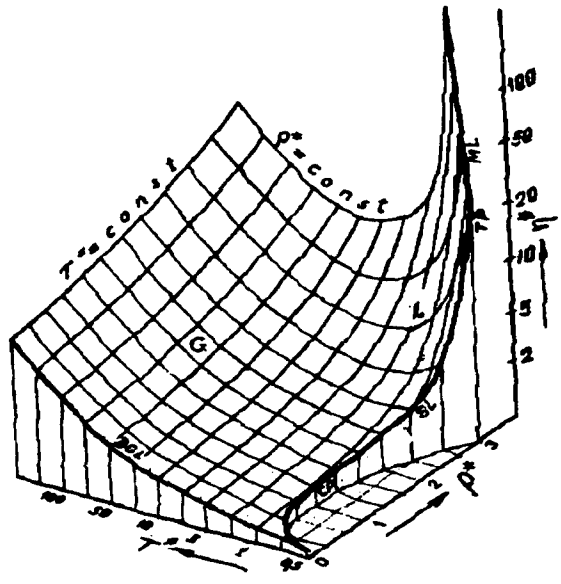

Fig. 5: Reduced viscosity $\eta^* = \eta/\eta_o$ in terms of reduced temperature, $T^* = T/T_c$ and density, $\rho^* = \rho/\rho_c$. G is the gas state; L is the liquid state; CP is the critical point; TP is the triple point; SL is the saturation line; ML is the melting line; DGL is the dilute gas limit

The investigation of viscosity and thermal conductivity in the regions of saturation and melting provides a means for extension into the range of extra-large pressures. Results obtained from fundamental theory studies are included as well into the treatment of data. Viscosity and thermal conductivity of the main components of interest (nitrogen, oxygen, hydrogen and water) are reviewed here. Experimental studies of the transfer coefficients for most matters are primarily limited to temperatures below *1000 – 1200 K* due to high chemical activities of the substances. Hence, the most extensive measurements of viscosity and thermal conductivity have been performed for less chemical active substances such as nitrogen or air. Generally, properties of the most chemical active molecule oxygen are less known. Table 2 gives a summary of the current boundaries of temperature and pressure of the experiment data for viscosity and thermal conductivity for some basic components.

	Viscosity				**Thermal conductivity**			
	Rarified Gas *0.1 MPa*	SL	Dense Gas		Gas, *0.1 MPa*	SL	Dense Gas	
	ΔT,K	*ΔT,K*	*ΔT,K*	*Δp, MPa*	*ΔT,K*	*ΔT,K*	*ΔT,K*	*Δp, MPa*
H_2	300-1000	14-32.976	to 1000	to 100	to 830	14-32*)	to 1000	to 100
N_2	400-2000	65-124	to 900	0.1-80	273-1373	65-124	300-430	to 10
		~126.5	~300	to 200			~300	0.1-1000
O_2	400-1960	55-150 ~70	300-525	0.1-80	300-1000	55-150	~300	to 360
Air	400-2000	70-128	300-523	0.1-80	300-1200	70-128	300-1200	0.1-100
							~300	to 360
H_2O	~1000	273.16-643.16	273-1000	0.1-80	~1000	273.16-643.16	~300	0.1-100

Table 2: Temperature and pressure limits reached in experimental investigations of viscosity and thermal conductivity

The recommended data for viscosity and thermal conductivity, as correlated tables data are included in the Standard Reference Data (GOST Standard, Russia, NIST Data and others) [4-6].
All major theoretical approaches in use for computing viscosity and thermal conductivity and diffusion at

high pressures are quasi-empirical. Due to the specific behavior of the transport properties at high densities it is recommended to perform predictions based on theoretical approaches only when experimental data is missing. Viscosity and thermal conductivity coefficients in the limiting case of zero density may be calculated applying Boltzmann equation and Chapman-Enskog method [7] using potential functions to account for particle interaction. Such data are suitable for comparison in wide ranges of temperature at low densities. The complementary data in the limit of the saturation line and the melting area may be important for correlation at high density.

Quasi-theoretical approaches

One of the wide-spread methods for the prediction of transport properties at high densities is a particular method of excess functions. Usually, the excess of viscosity and thermal conductivity is represented by a power low [8,9]. The main suggestion is that the expression for the viscosity or thermal conductivity coefficient consists of the two terms, with one of them a function of temperature and the other a function of density:

$$\eta(T,\rho)=\eta_o(T)+\Delta\eta\ (\rho) \tag{1}$$

$$\lambda(T,\rho)=\lambda_o(T)+\Delta\lambda(\rho) \tag{2}$$

The usual practice is to express the excessive values of $\Delta\eta\ (\rho)$ and $\Delta\lambda(\rho)$ in terms of a serial expansion of density:

$$\Delta\eta(\rho)=a_1\rho+a_2\rho^2+a_3\rho^3+a_4\rho^4+a_5\rho^5 \tag{3}$$

$$\Delta\lambda(\rho)=b_1\rho+b_2\rho^2+b_3\rho^3+b_4\rho^4+b_5\rho^5 \tag{4}$$

Although some results of the correlations (1)-(4) are in good agreement with experiments, the method of excess function holds only within certain limits. In reality, the functions $\Delta\eta\ (\rho)$ and $\Delta\lambda(\rho)$ are derived for either normal or large temperatures and do not hold for small temperatures and high densities. The method of excess viscosity or thermal conductivity yields reliable results only in the region of equidistant isotherms. But this equidistance is lost at high density and at low temperatures near the critical area. The isotherms of the reduced viscosity of hydrogen are shown in Figure 6. It can be seen that the error near the critical range may exceed 40%.

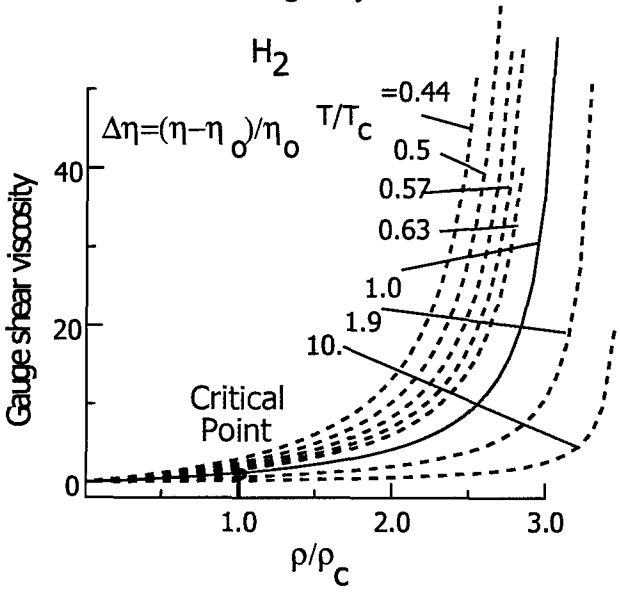

Fig. 6: Excess viscosity of Hydrogen reduced to dilute gas limit in terms of reduced of density.

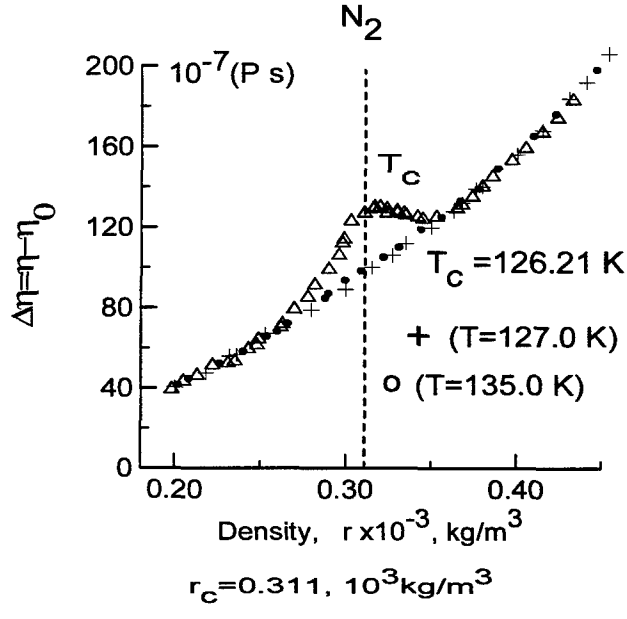

Fig. 7: Excess viscosity of Nitrogen near critical point

The behavior of the excess viscosity of nitrogen near the critical area is shown in Figure 7. The enhancement of the viscosity along the critical isotherm above the regular part is about 37%. Despite these shortcomings, it is obvious that the method of excess functions is quite useful in some cases.

Generalization on the base of Enskog equation

There are a variety of models proposed in the form of reduced density and reduced temperature. The most reasonable equations for the prediction of properties in wide areas of temperatures and pressures usually base on modifications of Enskog kinetic theory for hard spheres. Among them a unique equation for viscosity has been proposed [10,11]. This single equation describes the viscosity of both diluted gases and liquids. The fitting parameters of the equation have been derived using the most recent data of viscosity of diluted gases, of the two phases on saturation line, near the melting line and for dense states. Details of study are omitted here.
The quasi-theoretical equation of viscosity includes two terms, a kinetic part and a collision part, as

$$\mu = \mu_{kin} + \mu_{col}, \tag{5}$$

with μ_{kin} the kinetic part and μ_{col} the collision part of the viscosity taking into account the different mechanisms of impulse transfer. These parts are functions of reduced temperature and density (ρ / ρ_S) with ρ_S the density of the dense gas on the line of melting.

A series of calculations using the proposed equation of viscosity have been performed and the results are compared with direct computer simulations. This comparison confirmed the validity of this quasi-theoretical equation [10,11]. A set of the results obtained is shown in Figures 8 - 10. While Figures 8a and 8b show the isobars and isochores of viscosity of H_2, Figures 9 and 10 present the isochores of the viscosity of N_2 and O_2, respectively. Generally, the deviations of the results are in almost all cases less than a few percent.

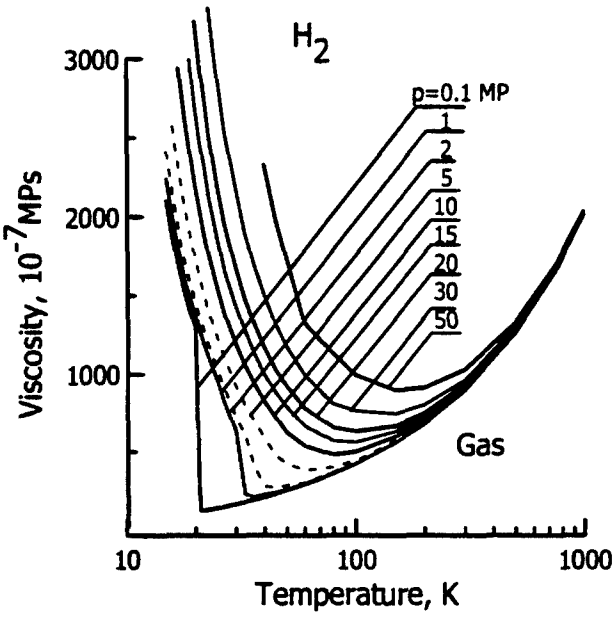

Fig. 8a: Viscosity isobars of H_2. Dotted lines are placed near critical pressure

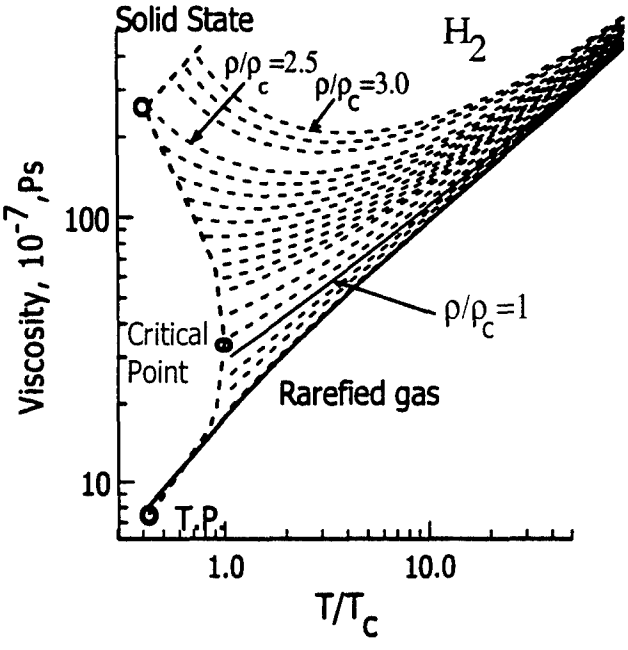

Fig. 8b: Viscosity isochores of H_2. Triplet Point (T.P.) and Critical Point (CP) are given on the saturation line

Model of the effective diameter sphere

Although the empirical correlation relies on direct experiments [11] is very useful and provides the basis for comparison and of reference, it cannot be applied for cases such as the dense states of H_2O or for mixtures of gases and liquids. Furthermore, a generalization of this correlation for other substances than the

experimentally investigated ones is questionable. Therefore, the only way of overcome these kind of difficulties is to predict the transport properties on the basis of kinetic theory.

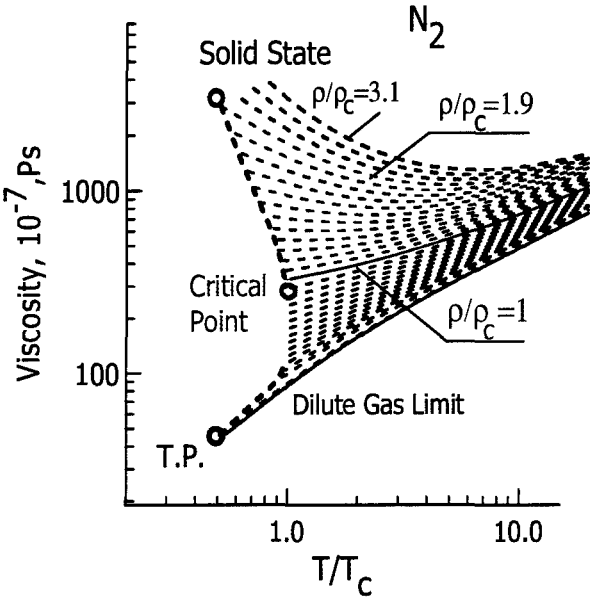

Fig. 9: Viscosity isochore of N_2.

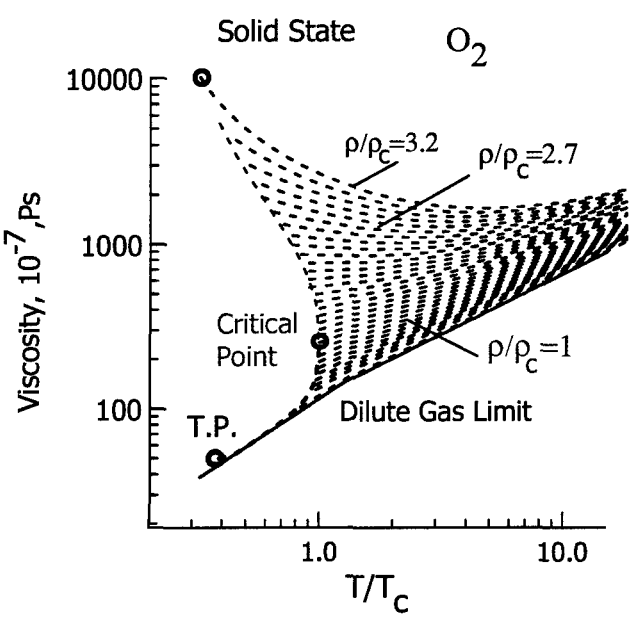

Fig.10: Viscosity isochore of O_2.

A novel model for the prediction of the viscosity of dense gases and liquids in a wide range of density and temperature is proposed [12-13], which bases on specific characteristics of particle interaction in a dense environment.

Both, the kinetic theory foundation and the generalization of the Enskog model for dense gases and fluids make use of the model of a hard sphere. They are unreliable for real fluids because the actual interactions between the particles are not taken into account. However, if the model of effective diameter of a sphere is applied properly using effective potential of the particle interaction, the transport properties of real fluids may be predicted successfully. The formalism of the Enskog hard sphere theory remains the same, but the real character of particle interaction is considered properly by the effective diameter σ_{ceff}.

Molecular dynamics (MD) [14-15] simulations show that the effective pair potential in dense media is a truncated function of the distance between the pairs due to a screening effect of neighboring particles. Therefore, the MD calculations were carried out based on the Lennard-Jones model with either a cut-off at some distance: $r \sim (2.5\text{-}3.0)\ \sigma_o$ or applying other modifications such as the (exp-6-8) truncated model.

Nevertheless, any truncation at a constant distance is valid only for liquids.

The Enskog equation of viscosity consists of two terms

$$\mu = \mu_{kin}(\sigma_{kin}) + \mu_{col}(\sigma_{col}), \tag{6}$$

with σ_{kin} the effective kinetic diameter (the parameter of impulse transfer along the particle's trajectory) and σ_{col} the effective collision diameter (the parameter of impulse transfer by the particles collision). At any temperature both parameters show systematic differences. Similar results are obtained for diffusion and thermal conductivity.

A new model of the effective kinetic diameter is proposed which assumes that this effective kinetic diameter is a function of temperature and density. This model describes the decrease of the free path of particles with increasing density. The interaction between particles is taken as Lennard-Jones (LJ) potential with a shielding function to account for environmental effects. The cut-off parameter is determined in terms of density and temperature and takes the overlapping of long-range attractive forces of closely packed of molecules into account.

We will describe the interaction of particles taking into account the overlapping of distance fields due to close molecular packing at higher densities taking the effective potential in form of a reference potential model with an exponential screening function

$$U(r) = \left[U_{rep}(r) + U_{att}(r)\right] \exp\left(-\left(\frac{r}{b_{cut}}\right)^2\right), \tag{7}$$

with b_{cut} the cut-off parameter, which accounts for screening interaction of the particles. The mean distance between the particles $s = n^{-1/3}$ is taken as a screening parameter. Thus,

$$b_{cut} = s \quad \text{or} \quad b_{cut} / \sigma_o = b_{cut}^* = (n\sigma_o^3)^{-1/3} = \left(n^*\right)^{-1/3}, \tag{8}$$

with n the number density, σ_o the parameter of the potential function (LJ in this case). In the case of low density the potential is transformed into the reference potential function.

The results of numerical simulation using the effective kinetic diameter coincide with the results of MD calculations for the limit of high density states as well as with kinetic diameter simulations of a dilute gas in the limiting case of DGL. For dense gases the effective kinetic diameter results show excellent agreement with results determined from viscosity experiments for argon, nitrogen and other gases.

For a given density, the effective kinetic diameter is derived from relation

$$\sigma_{kin}(T^*, b\rho) = \left[\Omega^{(2,2)}(T, b_{cut})\right]^{1/2} = \sigma_0\left[\Omega^{(2,2)*}(T^*, n^*)\right]^{1/2}, \quad b\rho = \frac{2}{3}\pi n^*, \tag{9}$$

with $\Omega^{(2,2)}$, the Ω-collision integrals of Cowling, b the volume of hard spheres .

The model of the effective kinetic diameter uses no empirical parameters and can therefore be applied for viscosity calculations when experimental data are missing. Since this approach accounts for density variations, it is most suited for property calculations with varying densities. The model can be used to predict transport properties of dilute gases, dense gases and liquids on the basis of a single equation.
A comparison of our predicted N_2 viscosities at *100 MPa* with data taken from the NIST is shown in Figures 11a and b show. The agreement between the direct theory (present calculation) and the correlation data (NIST) is quite reasonable. The increase of the deviation with decreasing temperature at very low temperatures may be related to the LJ reference potential function whose parameters are not reasonably suited for low temperatures.

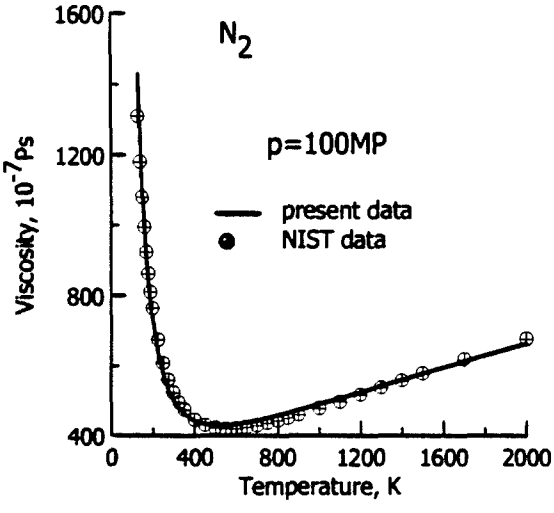

Fig. 11-a: Viscosity on N_2 : present calculation (solid curve) and NIST data (circles)

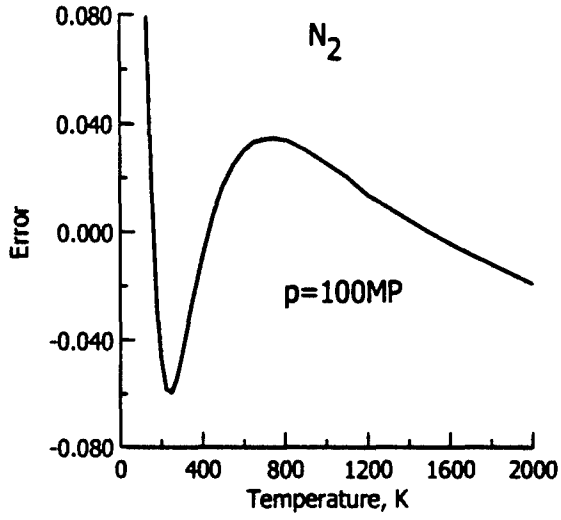

Fig. 11-b: Error of viscosity, $\Delta=[\eta(present)-\eta(NIST)]/\eta(present)$

Thermal non-equilibrium processes

The main processes in cryogenic liquid rocket engine systems are droplet vaporization and spray combustion including liquid jet atomization, spray formation, vaporization, multiphase flow mixing, ignition and combustion in a high pressure high temperature environment. The time scales of liquid jet atomization, evaporation, convection and mixing are such that oxygen droplets may penetrate into the flame front and enter the reactant which is mainly superheated steam for the propellant combination LOX/GH_2.

Any evaporation process involves heat and mass transfer from the hot surrounding gases to the droplet surface and vice versa. For an accurate prediction of these fluxes transport coefficients and thermodynamic properties of both fluids are needed. However, investigations have shown that not only conservation equations, equation of state (EQS), transport and thermodynamic properties must be modeled accurately, but also interface processes have to be taken into account. Typically, thermal equilibrium conditions on the droplet interface is assumed which may not hold at very large temperature and concentration gradients. Therefore, a model, which accounts for thermal non-equilibrium at the droplet surface, is necessary.

When the radius r of a spherical droplets is small and comparable with the mean free path λ of the molecules in the surrounding gas ($0.01 < Kn < 0.2$, $Kn=\lambda/2r$) the discrete molecular structure is considered in a slip-flow regime. Foundations of the basic Boltzmann equation are valid for small Kn numbers, and the Navier-Stokes equations (the governing equations for continuum) may be used for all the entire regime except the layer close to the interface. This Knudsen layer is specified as collisionless molecular flow regime. Its thickness is of the order of the mean free path of the molecules and therefore, the individual behavior of the molecules has to be considered. One way of correct simulation of the flow in the entire domain is to extrapolate the boundary conditions. The boundary conditions on the solid surface under continuum assumptions are modified by jump conditions of thermodynamic and gasdynamic values. The linear extrapolation of the real temperature field to the surface gives the unknown boundary ambient gas temperature $T_e\ (0)$ as shown in Figure 12.

The solution of Navier-Stokes energy equation with this boundary condition $T_e\ (0)$ coincides with the true solution outside the Knudsen layer. The difference between the liquid surface temperature T_{in} and the extrapolated gas temperature $T_e\ (0)$ on the surface $\Delta T_j = T_{in} - T_e\ (0)$ is the temperature jump. The same assumption is taken for concentrations of evaporated components. Accordingly, the difference $\Delta Y = Y_g^1 - Y_d^1$ is the concentration jump.

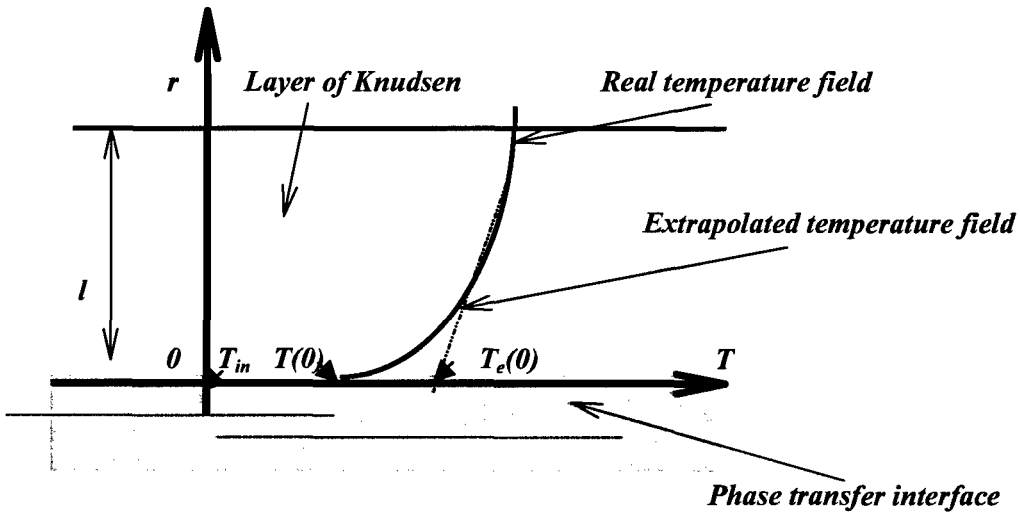

Figure 12: Schematic of temperature distribution around a droplet

We will consider here a model for single drop evaporation in a stagnant environment in an infinite volume. The special problem of the vaporization processes of liquid oxygen droplet (LOX) in superheated steam (GH_2O) is investigated. The conservation equations are used for oxygen droplet evaporating in steam under the following conditions: droplet radius ~ $10 \div 100\mu m$, temperature ~ $1500 \div 2000\ K$ and pressure $1 \div 10\ MPa$. Knudsen number falls in the range $0.01 < Kn < 0.15$. Since there are large gradients of

temperature and concentrations on the droplet surface, the boundary conditions for conservation equations must be investigated.

Droplet evaporation modeling of LOX in water steam (GH_2O) has some specific characters. The critical parameters of H_2O are considerable higher as compared to O_2. If surface temperature of the droplet is lower than *100 K* then according to the phase-equilibrium concept, the water vapor around the droplet condenses and freezes at its surface. However, an ice layer on a LO_2 droplet has never been observed so far in experiments. Evidently, the processes in the ultimate boundary layer of LO_2 and GH_2O may be in thermal non-equilibrium [16-18].

Model of quasi steady – state vaporization

If the characteristic time of molecular transfer is smaller than characteristic time of droplet evaporation, than the fields of temperature and concentration are invariant at constant droplet radius, and the quasi steady – state vaporization model may be used. It includes the following assumptions:

- the temperature of droplet is constant, uniform and equal to the wet-bulb temperature, i.e. droplet heating is neglected;
- the ambient gas has negligible solubility in the liquid and only oxygen diffuses from the surface;
- the radial motion of the liquid surface is assumed to be small;
- the pressure is equal to the ambient pressure everywhere;
- radiation, Dufour and Soret effects are negligible;
- density of gas phase is constant.

The governing system of equations is simplified further neglecting diffusion of the gas into the liquid droplet, chemical reactions and viscous dissipation. To determine the temperature and concentration jumps, Yalamov's approach is applied [19 – 21].

The resulting simplified system of equations is as follows [22 – 23]

$$R_u T = \left(p + \frac{a(T)}{V(V+b)} \right)(V-b), \tag{10}$$

$$v\frac{dY_1}{dr} = \frac{1}{r^2 \rho_m}\frac{\partial}{\partial r}(\rho_m D_{12} r^2 \frac{dY_1}{dr}), \tag{11}$$

$$\frac{1}{r^2}\frac{\partial}{\partial r}(r^2 \rho_m v) = 0, \tag{12}$$

$$\rho_m C_V \frac{d\ T}{dr} = \frac{1}{r^2}\frac{d}{dr}\left(r^2 \lambda_m \frac{dT}{dr} \right) + \left(C_{V_1} - C_{V_2} \right)\rho_m D_{12} \frac{dY_1}{dr}\frac{dT}{dr} - \frac{p}{r^2}\frac{d}{dr}(r^2 v). \tag{13}$$

The boundary conditions for the gas phase are as follows:

For $r = r_d$:

$$\rho_m v = j,\ Y_1 v - D_{12}\frac{dY_1}{dr} = j\frac{1}{\rho_m}, \tag{14}$$

$$\lambda_m \frac{dT}{dr} = jl, \tag{15}$$

$$(T_e^g - T_d^l)\,|_{r=r_d} = K_T^{(T)} \frac{\partial T^g}{\partial r}\,|_{r=r_d} + K_T^{(n)} T_\infty \frac{\partial Y_1}{\partial r}\,|_{r=r_d},$$
$$\left(Y_e^g - Y_1^d\right)|_{r=r_d} = K_n^{(n)} \frac{\partial Y_1}{\partial r}\,|_{r=r_d} + \frac{K_n^{(T)}}{T_\infty} \frac{\partial T^l}{\partial r}\,|_{r=r_d} \qquad (16)$$

For $r = \infty$:

$$\mathrm{T} = \mathrm{T}_0, \mathrm{Y}_1 = Y_{1\infty}. Y_1 = \frac{\rho_1}{\rho_m},\ \rho_\mathrm{m} = \rho_1 + \rho_2,\ \mathrm{R} = \mathrm{Y}_1 R_1 + (1 - Y_1) R_2, \mathrm{C_V} = Y_1 C_{V_1} + (1 - Y_1) C_{V_2}. \qquad (17)$$

T_e^g, Y_e^g are temperature and concentration of oxygen in the gas phase on the droplet surface; T_d^l, Y_1^l are temperature and concentration of oxygen in the liquid on the droplet surface. ρ_m is the mass density of the mixture, v the radial velocity; Y_i, D_{12} are the mass fraction and the binary diffusion coefficients for each species, S_y is a term which stands for different effects, for example, Dufour, Soret effects, inertia source term ,etc..; h_m, h_i are the mixture and the specific enthalpies, λ_m is the thermal conductivity of the mixture; $\Delta\overline{H} = \overline{h}_1^{vap} - \overline{h}_1^{liq}$ is the specific enthalpy of vaporization of species ; $K_T^{(T)}, K_n^{(n)}$ are coefficients of temperature and concentration jumps, $K_T^{(n)}, K_n^{(T)}$ cross coefficients.

Furthermore, we will introduce the following the non - dimensional parameters:

$$\xi = \frac{r}{r_0},\ \theta = \frac{\mathrm{T}}{\mathrm{T}_0},\ \delta = \frac{\rho}{\rho_0},\ \mathrm{L} = \frac{1}{\mathrm{R}_0 T_0},\ \Lambda = \frac{\lambda_\mathrm{m}}{\mathrm{p}_0 R_0 D_{12_0}},\ \overline{\mathrm{D}} = \frac{\mathrm{D}_{12}}{\mathrm{D}_{12_0}},$$
$$R_0 = (1 - Y_{10}) R_2 + Y_{10} R_1,\ \overline{\mathrm{R}}_\mathrm{i} = \frac{R_i}{R_0},\ \mathrm{C}_{\mathrm{p}_\mathrm{i}} = \frac{C_{p_i}}{R_0},\ \mathrm{C}_\mathrm{p} = \frac{C_p}{R_0},\ \overline{\mathrm{p}} = \frac{\mathrm{p}}{\mathrm{p}_0}, \qquad (18)$$
$$C_V = C_p - \overline{R},\ \eta = \frac{1}{\xi},\ \overline{R}_e = (1 - Y_e^g)\overline{R}_2 + Y_e^g \overline{R}_1$$

After integration of the system of governing equation and some additional mathematical simplifications an analytical solution of the steady - state evaporation problem is derived. The equations for the temperature

$$A(1-\theta) + \left(B + \frac{\gamma_1}{\gamma_0} A\right) ln \frac{\gamma_0 - \gamma_1}{\gamma_0 \theta - \gamma_1} = \gamma_0 \eta, \qquad (19)$$

$$\gamma_0 = J\left(C_{V_1} + \overline{R}_2\right),\ \gamma_1 = \theta_d \gamma_0 - LJ, \qquad (20)$$

$$\lambda_m = AT + B. \qquad (21)$$

and concentration distributions

$$\frac{\overline{D}}{\overline{R}\Lambda\theta} \frac{dY_1}{d\theta} = \frac{1 - Y_1}{\left(C_{v_1} + \overline{R}_2\right)(\theta_d - \theta) - L} \qquad (22)$$

can be integrated analytically for $\overline{D} = const$:

$$\frac{1}{\overline{R}_1} ln \frac{[Y_1\overline{R}_1 + (1-Y_1)\overline{R}_2](1-Y_{1\infty})}{(1-Y_1)} = \frac{A}{\overline{D}(C_{V_1} + \overline{R}_2)}$$
$$\left\{\frac{1}{2}\left(1-\frac{\gamma_1}{\gamma_0}\right)^2 - \frac{1}{2}\left(\theta-\frac{\gamma_1}{\gamma_0}\right)^2 + \left(2\frac{\gamma_1}{\gamma_0}+\frac{B}{A}\right)(1-\theta) + \frac{\gamma_1}{\gamma_0}\left(\frac{\gamma_1}{\gamma_0}+\frac{B}{A}\right) ln \frac{\gamma_0-\gamma_1}{\gamma_0\theta-\gamma_1}\right\}. \quad (23)$$

For the power dependence of $\overline{D}$ on temperature, the analytical solution depends on the power of temperature. For $D = D_0\left(\frac{T}{T_0}\right)^{1.75}$ the equation for concentration distribution can be written as

$$\frac{1}{\overline{R}_1} \ln \frac{[Y_1\overline{R}_1 + (1-Y_1)\overline{R}_2](1-Y_{1\infty})}{(1-Y_1)} = \frac{4A}{B}\left(\theta^{1/4} - \theta_e^{1/4}\right) - \frac{2}{B\xi^3}(Ac+B)\cdot\left\{\frac{1}{2}\ln\left|\frac{\xi+\theta^{1/4}}{\xi-\theta^{1/4}}\right| + arctg\frac{\theta^{1/4}}{\xi}\right\}\Bigg|_{\theta_e}^{\theta} \quad (24)$$

with

$$\xi = \left(\theta_e - \frac{L}{C_{V_1} - \overline{R}_2}\right). \quad (25)$$

This system of the algebraic equations for the temperature and concentration fields in the neighborhood of the droplet is closed by the expressions for θ_e , Y_e^g, which are determined from the temperature and jumps conditions.

Finally the system of algebraic equations for determination T_e^s, Y_e^g, Q^m is the following

$$(T_e^g - T_d^l)\Big|_{r=r_d} = -K_T^{(T)}\left(\frac{Q^T - Q^m h_1}{4\pi r_d^2 \lambda_e}\right) + K_T^{(n)} T_\infty \left(\frac{Q^m(1-Y_e^g)}{4\pi r_d^2 \rho_m D_{12}}\right),$$
$$\left(Y_e^g - Y_1^d\right)\Big|_{r=r_d} = K_n^{(n)}\left(\frac{Q^m(1-Y_e^g)}{4\pi r_d^2 \rho_m D_{12}}\right) - \frac{K_n^{(T)}}{T_\infty}\left(\frac{Q^T - Q^m h_1}{4\pi r_d^2 \lambda_e}\right) \quad (26)$$

$$Q^m = \frac{4\pi r_d}{(l-h_1)}\left[B\left(T_e^g - T_0\right) + \frac{A}{2}\left(T_e^{g2} - T_0^2\right)\right], \quad Q^T = lQ^m, \quad (27)$$

with Q^m, Q^T, the integral mass and heat fluxes and l the heat of evaporation.

To calculate the concentration and temperature jumps according to Yalamov and co-workers [21] we simplify the jumps coefficients, as given below:

$$K_T^{(T)} = \Psi_1^{(0)} \frac{\lambda}{2\, kn_0 \Delta_{1/2}} \left(\frac{\pi}{2kT_0}\right)^{\frac{1}{2}} \quad (28)$$

$$K_T^{(n)} = \Psi_2^{(a)} \frac{n_0^2}{n_{01} n_{02}} \left(\frac{m_1}{2kT_0} \right)^{1/2} D_{12} - \frac{n_0^2 (m_1 + m_2)}{4 \rho_0^2 \gamma_0} \left(\frac{\pi}{2kT_0} \right)^{1/2} \times \left(m_2^{3/2} - m_1^{3/2} \right) \left(D_{12} - D_{12}^{[1]} \right) \left(\frac{104}{25\pi} \right) \tag{29}$$

$$K_n^{(n)} = \Psi_3^{(a)} \frac{n_0^2}{n_{01} n_{02}} \left(\frac{m_1}{2kT_0} \right)^{1/2} D_{12} + \left[\frac{4 n_0^2 (m_1 + m_2)}{5 \rho_0 n_{01} \gamma_0} \left(\frac{m_1}{2kT_0} \right)^{1/2} \right] \times \times \left(D_{12} - D_{12}^{[1]} \right) \tag{30}$$

$$K_n^{(T)} = -\Psi_1^{(a)} \frac{\lambda}{2kT \Delta_{-\frac{1}{2}}} \left(\frac{\pi}{2kT_0} \right)^{1/2} - \frac{26}{25} \frac{n_{02}}{\rho_0^2} \frac{(m_1 + m_2)(m_2^{3/2} - m_1^{3/2}) \lambda}{k \gamma_0 \sqrt{2\pi k T_0}} \times \times \left(\frac{\left(D_{12} - D_{12}^{[1]} \right)}{D_{12}} \right) \tag{31}$$

$$\Delta_{-1/2} = \frac{n_{01}}{n_0} m_1^{-1/2} + \frac{n_{02}}{n_0} m_2^{-1/2}, \quad \Delta_{1/2} = \frac{n_{01}}{n_0} m_1^{1/2} + \frac{n_{02}}{n_0} m_2^{1/2}, \quad \gamma_0 = \left(1 - \frac{2}{5} \frac{\Omega_{12}^{(1,2)}}{\Omega_{12}^{(1,1)}} \right)^{-1} \tag{32}$$

$$\Psi_1^{(a)} = \frac{1}{2} + \frac{52}{25\pi} + \left(\frac{52}{25\pi} \right) \frac{n_{01} n_{02} \left(m_1^{3/2} - m_2^{3/2} \right)}{\rho_0^2 \sqrt{m_1 m_2}}, \tag{33}$$

$$\Psi_2^{(a)} = -\left(2 - \frac{5}{2} \right) \times \frac{n_{01} \sqrt{\pi}}{4 n_0 \Delta_{-1/2} m_1^{1/2}} + \frac{2}{5} \frac{\rho_{01}}{\rho_0 \sqrt{\pi}}, \tag{34}$$

$$\Psi_3^{(a)} = \left(2 - \frac{5}{2} \right) \times \frac{n_{01} \sqrt{\pi}}{8 n_0 \Delta_{-1/2} m_1^{1/2}} + \frac{2}{\sqrt{\pi}} - \frac{2 \rho_{01}}{5 \rho_0 \sqrt{\pi}} + \left(\frac{1}{2} \right) \sqrt{\pi}, \tag{35}$$

$$\Psi_4^{(a)} = \frac{3}{4} + \frac{52}{25\pi} + \left(\frac{52}{25\pi} \right) \frac{n_{01} n_{02} \left(m_1^{3/2} - m_2^{3/2} \right)}{\rho_0^2 \sqrt{m_1 m_2}} - \frac{4}{5} \frac{n_0 m_1^{3/2}}{\rho_0 \pi} \Delta_{-1/2} \tag{36}$$

with n_0 - molecular mixture concentration, n_{0i} - molecular concentration of i^{th} component, $n_0 = n_{01} + n_{02}$, m_i - mass of a molecule; D_{12} - coefficient of binary diffusion, $D_{12}^{[1]}$ - coefficient of binary diffusion first approach; k - Boltzmann constant; T_0 - temperature of a droplet and $\Omega_{ij}^{(l,s)}$ - collision integrals.

The radius of evaporating droplet is determined by equation

$$r^2 \frac{dr}{dt} = -\frac{Q^m}{4\pi \rho_l}. \tag{37}$$

After integrating

$$r\frac{dr}{dt} = -\frac{1}{(l-h_1)\rho_l}\left[B\left(T_e^g - T_0\right) + \frac{A}{2}\left(T_e^{g^2} - T_0^2\right)\right], \tag{38}$$

$$r_o^2 - r_d^2 = -\frac{2}{(l-h_1)\rho_l}\left[B\left(T_e^g - T_0\right) + \frac{A}{2}\left(T_e^{g^2} - T_0^2\right)\right]\Delta t \tag{39}$$

follows.

Numerical results

A series of computations have been performed to investigate the influence of various physical phenomena on the distributions of the temperature and the concentration. We computed concentration and temperature jumps on the surface of an evaporating single oxygen droplet in steam for initial droplet radii of *10, 25* and *50 μm* for $T = 1500 \div 2500K$ and $P = 0.1$ *and 4 MPa.*

It is found that the initial droplet size as well as the pressure and temperature of the surroundings have a significant influence on the droplet behavior [17]. Due to the lack of experimental data for the binary system LOX/GH_2O we have tested the model comparing our results with experimental data [24] for the system LOX/N_2, see Figure 12. The results are in a good agreement. The predicted lifetimes of LOX droplets in steam for various pressures and steam temperatures are shown in Figure 13 for different initial droplet radii.

The temperature jumps on the boundary surface of droplet and surroundings were computed using different assumptions about thermodynamic and transport properties behavior. The physical properties in terms of temperature and density were taken in the first case. In a second case, the averaged mean values were used [18]. The corresponding temperature jumps on the droplet surface are demonstrated in Figures 14a,b for different droplet radii and two ambient pressures $p = 0.1$ and *4 MPa* at various initial steam temperatures T_o. It is evident from the figures that the usage of simple approximations for the thermodynamic and transport properties may cause significant errors.

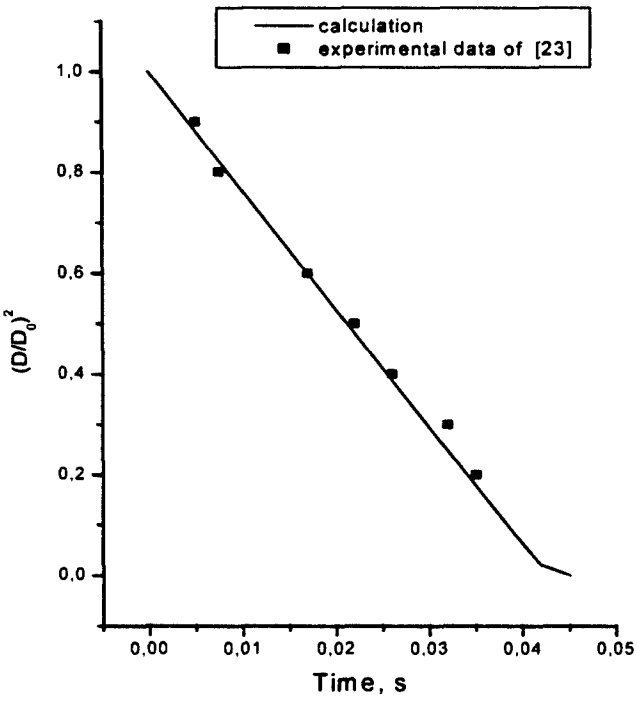

Fig. 12: Averaged Variation of $(D/D_0)^2$ over time for the system LOX/N_2; $P = 0.1$ *MPa,* $T_{N2} = 300K$

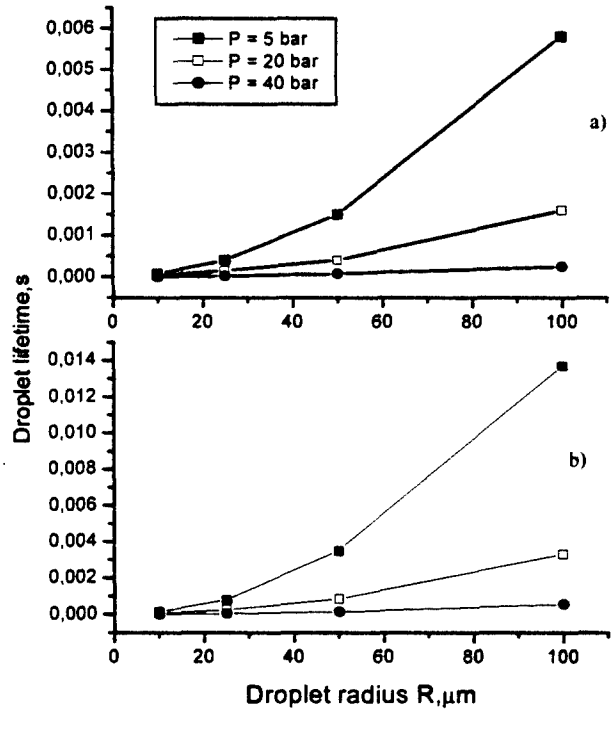

Fig. 13: Droplet lifetime over initial droplet radius for the system LOX/GH_2 for various pressures and initial steam temperatures
a) T_{GH2O}=*1500 K* and b) T_{GH2O}=*1000 K*

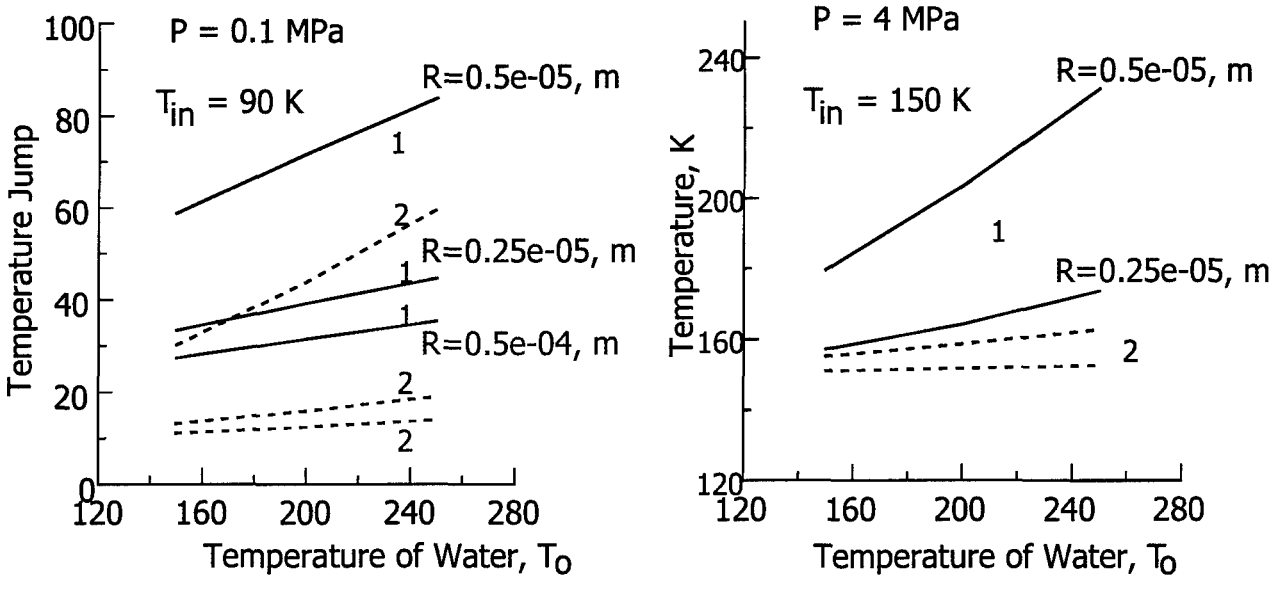

Fig. 14 a,b: Temperature jumps on the boundary surface of droplet and surroundings for a) $P = 0.1$ *MPa*, $T_{in} = 90$ *K* and b) $P = 4$ *MPa*, $T_{in} = 150$ *K*: Solid curves (1) are the computations with real properties; dotted curves (2) are the computations with averaged constant properties at various droplet radii R. T_0 is the initial temperature of surroundings, T_{in} is the temperature of liquid droplet surface

Conclusions

It has been shown that viscosity and thermal conductivity of fluids strongly depend on density and temperature and that the prediction of transport properties which bases on simple models of power expansion of density yield erroneous results if applied beyond certain limits. The proposed effective kinetic diameter model makes it possible to describe the viscosity of liquids and gases in wide ranges of temperature and density. The performed numerical studies confirmed that the new model is the less computing resources compared with the MD simulations, which requires many hours of computations per individual data point and many days for mixtures. Computations, which base on the effective kinetic diameter model, can be done with less effort.

The vaporisation model which accounts for thermal non-equilibrium boundary conditions at the droplet surface and describes thermodynamic processes on the interface more accurately but relies heavily on exact transport properties.

References

[1] N.B. Vargaftic. Handbook. Thermo-Physical Properties of Gases and Liquids. Moscow, Nauka., 1972.

[2] V.N. Zubarev, A.D. Kozlov, V.M. Kuzneszov, L.V. Sergeeva, et.al. Handbook. Thermophysical properties of industrial important gases at high pressures and high temperatures, Moscow, Energoizdat. 1989.

[3] NIST. Thermo-physical properties of pure fluids Database, Original development by R.D. McCarty and V.App, NBS Technical Note 1097. May 1986.

[4] J.O. Hirschfelder, C.F. Curtis, R.B. Bird, Molecular Theory of Gases and Liquids, New York, Wiley, 1954.

[5] Nitrogen. Viscosity and thermal conductivity coefficients at temperatures 65-1000K and pressures from limiting dilute gas to 200 MPa. SCSD 89-85. State Committee on Standard DATA. Standard and Reference Data TABLES. Moscow.

[6] Oxygen. Viscosity and thermal conductivity coefficients at temperatures 70-500K and pressures from limiting dilute gas to 100 MPa. SCSD 93-86. State Committee on Standard DATA. Standard and Reference Data TABLES. Moscow.

[7] Normal Hydrogen. Viscosity and thermal conductivity coefficients at temperatures 14-1500K and pressures from limiting dilute gas to 100 MPa. SCSD 182-87. State Committee on Standard DATA. Standard and Reference Data TABLES. Moscow.

[8] N.B. Vargaftic, L.P. Filippov, A.A. Tarzimanov, E.E. Tozskiy. Handbook on the Thermo-conductivity of Liquids and Gases. Moscow, Energoizdat. 1990.

[9] R.C. Reid, J.M. Prausnitz, B.E. Poling. The Properties of Gases and Liquids. 4th Ed. McGraw Hill, New York, 1987.
[10] E. Liousternik, M.P.Voronin. Universal equation for viscosity of liquids and gases. Thermo-Physics of High Temperatures, V.21, N3, 1983.
[11] M.P. Voronin. Mathematical description diagram of viscosity. Ph.D. Thesis, IHT, Moscow, 1984.
[12] I.A. Sokolova, V.E. Liousternik. Model and Simulation Method for Study of Dense Fluids. Shock Compression of Condensed Matters - 1995. Proceedings of the Conference of the APS Topical Group on Shock Compression of Condense Matters. Seattle, Washington, 1995. Ed. S.C. Shmidt. W.C. Tao. AIP Conference Proceedings. 370. Part 1., 1996., p.167-170.
[13] I.A. Sokolova, V.E. Lusternik. Numerical analysis of density dependence for effective transport kinetic diameter for real fluids. Lecture Notes in Computer Science. V.1196, Springer-Verlag, 1997. Eds: L.Vulkov, J.Wasniewski, P.Ya., p. 474-481.
[14] M. Schoen, C. Hoheisel. The shear viscosity of a Lennard-Jones fluid calculated by equilibrium MD. Molec. Physics. 1985. V.53, N3., p.653
[15] J.J. Erpenbeck. Transport coefficients of hard-sphere mixtures. III. Diameter ratio 0.4 and mass ratio 0.03 at high fluid density. Physical Review E. V.1993. 48, N1, p.223-232.
[16] Slavinskaya N.A., Haidn O. J., O_2 -H_2O vapor–liquid phase equilibria, Proc. of Spray 99, Bremen, 1999.
[17] N.A. Slavinskaya, O.J. Haidn. Numerical modeling of isolated oxygen droplet evaporation in steam: A First approach, Proc. of 16th ILASS Europe, Darmstadt, Germany, 2000.
[18] N.A. Slavinskaya, O.J. Haidn. Numerical modeling of liquid oxygen evaporation in steam using non-equilibrium boundary conditions, AIAA 2001-0335, 2001.
[19] S.K. Loaylka. Temperature jump in a gas mixture. Phys. of Fluids, 1974, vol. 17, No. 15, p.897.
[20] C. Shen. The concentration - jump coefficient in a rarefied binary gas mixture. J. Fluid Mech., 1983, vol. 137, pp. 221-231.
[21] I.Y. Yalamov, V.S. Galojan. The droplet's dynamic in azeotropic viscosity medium. Erevan, Luis, 1985.
[22] I.K. Rakhmatulina. The investigation of non - steady heat transfer under evaporation, condensation and burning of drops. Ph.D., Institute of Mechanics of Lomonosov Univ., 1977.
[23] T. Elperin, B. Krasovitov. Radiation, thermal diffusion and kinetic effects in evaporation and combustion of large and moderate size fuel droplets, Int. J. Mass Transfer, 1995, Vol. 38, N 3, pp. 409-418
[24] X. Chesneau, C. Chauveau, I. Gökalp. Experiments on high pressure vaporization of liquid oxygen droplets. AIAA-94-0688, 1994.